



ELSEVIER

Available online at www.sciencedirect.com

SCIENCE @ DIRECT®

Physica A 325 (2003) 361–370

PHYSICA A

www.elsevier.com/locate/physa

Different regimes of synchronization in nonidentical time-delayed maps

C. Masoller^a, Damián H. Zanette^{b,*}

^a*Instituto de Física, Facultad de Ciencias, Universidad de la República, Igúá 4225, Montevideo 11400, Uruguay*

^b*Consejo Nacional de Investigaciones Científicas y Técnicas, Centro Atómico Bariloche (CNEA), Instituto Balseiro (UNC), 8400 Bariloche, Río Negro, Argentina*

Received 22 March 2002

Abstract

We study the synchronization of time-delayed nonidentical maps subject to unidirectional (master–slave) coupling. The individual dynamics of the maps have a delay n_1 , and the coupling acts with a delay n_2 . We show analytically that, suitably tuning the slave map parameters, two distinct synchronization regimes can occur. In one regime, the lag time between the slave and the master maps is given by the delay of the coupling, n_2 , while in the other regime is given by the difference between the delays, $n_1 - n_2$. We analyze the effect of the coupling strength on the different synchronization regimes in logistic and Hénon maps.

© 2003 Elsevier Science B.V. All rights reserved.

PACS: 05.45.Xt; 05.65.+b

Keywords: Chaos synchronization; Time-delayed systems

1. Introduction

Delay differential equations have received much attention over the years because of the significant role of delayed feedback in the dynamics of many physical and biological systems [1]. On the one hand, delay-differential systems often exhibit multistability—i.e., the coexistence of several attractors—and multistability enables such systems to act as memory devices [2,3], an idea first suggested by Ikeda and Matsumoto [4]. On the other, the study of delay systems is motivated by the fact that these systems exhibit

* Corresponding author. Tel.: +54-2944-445173; fax: +54-2944-445299.

E-mail addresses: cris@fisica.edu.uy (C. Masoller), zanette@cab.cnea.gov.ar (D.H. Zanette).

high-dimensional chaos and, therefore, can be used in communication systems based on chaotic synchronization, to securely encrypt information into their chaotic outputs [5,6].

Recently, Voss [7] discovered an interesting regime of synchronization of time-delayed systems, the so-called ‘anticipating synchronization’ regime. In this regime, the slave system becomes synchronized to the chaotic future state of the master system. The equations considered in Ref. [7] for the master, x , and slave, y , systems are

$$\begin{aligned}\dot{x} &= -\alpha x + f(x_\tau), \\ \dot{y} &= -\alpha y + f(x)\end{aligned}\quad (1)$$

with $x_\tau \equiv x(t - \tau)$ and f a nonlinear function. The synchronization manifold is $y(t) = x(t + \tau)$ and it was shown that due to the interplay of memory effects and relaxation mechanisms it can be globally stable. This regime of synchronization has attracted a lot of attention, numerically and experimentally, in the context of unidirectionally coupled semiconductor lasers with optical feed-back from an external mirror [8–14]. Also in Ref. [15], Voss studied the regime of anticipating synchronization for non-time-delayed systems. The equations for the master, x , and for the slave, y , systems were

$$\begin{aligned}\dot{x} &= f(x), \\ \dot{y} &= f(y) + \eta(x - y_\tau),\end{aligned}\quad (2)$$

where $y_\tau \equiv y(t - \tau)$ and η measures the strength of the coupling. While in the coupling scheme, Eq. (1) the lag-time between the two systems is equal to the delay-time of the master system (and therefore can be arbitrarily large), in the coupling scheme (2) the lag-time between the two systems cannot be too large for the synchronization manifold $y(t) = x(t + \tau)$ to be globally stable [15].

In a previous work, we studied the regime of anticipating synchronization in two chaotic *identical* maps with unidirectional (master–slave) coupling [16]. The equations for the master, x , and for the slave, y , maps were

$$\begin{aligned}x_{n+1} &= bx_n + f(x_{n-n_1}), \\ y_{n+1} &= by_n + (1 - \eta)f(y_{n-n_1}) + \eta f(x_{n-n_2}),\end{aligned}\quad (3)$$

where b is a parameter that represents a relaxation mechanism ($|b| < 1$), f is a nonlinear function that has the form of a time-delayed feedback with delay n_1 (notice that the master and slave maps have the same intrinsic delay n_1), and the parameter $\eta \in [0, 1]$ measures the strength of the coupling that acts with a delay n_2 . If $\eta = 0$ the maps are uncoupled, while if $\eta = 1$ the equation for the slave map becomes $y_{n+1} = by_n + f(x_{n-n_2})$ and there is a complete replacement of the slave variable in the nonlinear function, as in Eq. (1). The synchronization manifold is $y_n = x_{n-n_2+n_1}$ and depending on the sign of the difference $n_1 - n_2$, the slave map can synchronize to a future or a past state of the master map. In Ref. [16], we studied analytically the stability properties of the synchronized state, and found that they are independent of the coupling delay n_2 . These results were compared with numerical simulations of a delayed map that arises from discretization of the Ikeda delay-differential equation [$f(x) = a \sin(x)$]. We showed that

in that case the critical value of the coupling strength above which synchronization is stable becomes independent of the delay n_1 for large delays.

In this paper, we study the synchronization of two chaotic *nonidentical* maps with unidirectional (master–slave) coupling. We consider a master, x , and slave, y , maps of the form

$$\begin{aligned}x_{n+1} &= \alpha f(x_n) + \beta f(x_{n-n_1}) + g(x_n), \\y_{n+1} &= \alpha_s f(y_n) + \beta_s f(y_{n-n_1}) + g(y_n) + \eta f(x_{n-n_2}),\end{aligned}\quad (4)$$

where α , β , α_s and β_s are parameters, and $\eta \in (-\infty, +\infty)$ is the coupling strength. We show analytically that, by suitably tuning the slave map parameters, (α_s, β_s) , two distinct synchronization regimes are, in principle, possible. In one regime, the lag-time between the slave and the master maps is given by the delay of the coupling, n_2 , while in the other regime is given by the difference between the delays, $n_1 - n_2$. We exemplify the results with numerical simulations of Logistic and Hénon maps.

The possibility of two different regimes of synchronization is a problem that has been studied by several authors in the context of unidirectionally coupled semiconductor lasers with optical feedback from an external mirror [17–23]. The results we find here for coupled maps (i.e., the existence of two different synchronization regimes with lag-times n_2 and $n_1 - n_2$) agree with those found previously for semiconductor lasers with optical feedback (where the lag-times are either the flight time from master laser to the slave laser, τ_c , or the difference $\tau - \tau_c$ where τ is the round-trip time in the external cavity).

However, we want to point out that there is a fundamental difference between the synchronization regimes in unidirectionally coupled maps and those in unidirectionally coupled lasers with optical feedback. While we show here that for coupled maps the two synchronization regimes are particular cases of synchronization when the slave map has two time-delayed terms, for semiconductor lasers this is not the case. For semiconductor lasers, due to the phase dynamics, the two synchronization regimes cannot be unified in a single framework, and they exhibit very different characteristics (different sensibility to noise, detuning and other parameter mismatches).

This paper is organized as follows. In Section 2, we define the two synchronization regimes. As an illustration, in Section 3 we present numerical simulations of Logistic and Hénon delayed maps. We show the parameter regions where the two synchronization regimes occur, and analyze the effect of the coupling strength on the synchronization regions. Finally, in Section 4 we present our conclusions.

2. Master–slave coupled delayed maps

We consider a generic master map of the form

$$x_{n+1} = \alpha f(x_n) + \beta f(x_{n-n_1}) + g(x_n), \quad (5)$$

where α and β are parameters. The slave map is given by

$$y_{n+1} = \alpha_s f(y_n) + \beta_s f(y_{n-n_1}) + g(y_n) + \eta f(x_{n-n_2}). \quad (6)$$

If the parameters of the slave map are tuned in such a way that $\alpha_s = \alpha$ and $\beta_s = \beta - \eta$ (case I), the slave map reduces to

$$y_{n+1} = \alpha f(y_n) + \beta f(y_{n-n_1}) + g(y_n) + \eta[f(x_{n-n_2}) - f(y_{n-n_1})]. \tag{7}$$

Full synchronization can be expected for sufficiently large η on the synchronization manifold $y_n = x_{n+n_1-n_2}$. On the other hand, if the parameters of the slave map are tuned in such a way that $\alpha_s = \alpha - \eta$ and $\beta_s = \beta$ (case II), the slave map reads

$$y_{n+1} = \alpha f(y_n) + \beta f(y_{n-n_1}) + g(y_n) + \eta[f(x_{n-n_2}) - f(y_n)] \tag{8}$$

and full synchronization may occur on the synchronization manifold $y_n = x_{n-n_2}$. Therefore, depending on the parameters of the slave map, α_s and β_s , full synchronization can take place with two different lag-times, $\Delta_I = n_2 - n_1$ in the case of Eq. (7) and $\Delta_{II} = n_2$ in the case of Eq. (8). Note that, in case I, one can have anticipated synchronization for $n_1 > n_2$ [7,9,15].

The actual possibility of observing full synchronization in either case is determined by the stability of the synchronized state. Linear stability analysis of Eqs. (7) and (8) can be carried out by noticing first that the two equations can be written in a unified form as

$$y_{n+1} = h(y_n) + \beta f(y_{n-n_1}) + \eta[f(x_{n-n_2}) - f(y_{n-n_3})], \tag{9}$$

with $h(y) = \alpha f(y) + g(y)$. In Eq. (7), we have $n_3 = n_1$, whereas in Eq. (8) we have $n_3 = 0$. The synchronization manifold is $y_n = x_{n+n_3-n_2}$. Applying a perturbation $y_n = x_{n+n_3-n_2} + \delta_n$, replacing in Eq. (9), and taking into account Eq. (5) we get, to the first order in the perturbation,

$$\delta_{n+1} = h'(x_{n+n_3-n_2})\delta_n + \beta f'(x_{n+n_3-n_2-n_1})\delta_{n-n_1} - \eta f'(x_{n-n_2})\delta_{n-n_3}, \tag{10}$$

where primes indicate derivatives. Eq. (10) can be formally integrated by introducing a linear $(N+1)$ -dimensional map, with $N = \max\{n_1, n_3\}$, for a variable $\mathbf{r}_n = (r_n^0, r_n^1, \dots, r_n^N)$, with $r_n^k = \delta_{n-k}$. This equivalent map is given by

$$\mathbf{r}_{n+1} = M_n \mathbf{r}_n, \tag{11}$$

where the elements of the matrix M_n are given by the (time-dependent) coefficients in Eq. (10) [16]. The solution to Eq. (11) reads

$$\mathbf{r}_n = U_n \mathbf{r}_0 = M_{n-1} M_{n-2} \dots M_1 M_0 \mathbf{r}_0, \tag{12}$$

so that the state of full synchronization is linearly stable if all the eigenvalues of the evolution matrix U_n vanish for $n \rightarrow \infty$. Whether this condition holds or not for a given value of the coupling constant η can be readily verified by numerical means. Note that all the elements of matrix M_n , given by the coefficients in Eq. (10), involve a delay n_2 which thus acts as a uniform time shift. This fact implies that, in the limit $n \rightarrow \infty$, the eigenvalues of U_n become independent of n_2 . Consequently, the value of n_2 is irrelevant to the stability of full synchronization (cf. Ref. [16]). Note carefully that, generally, full synchronization for the two cases considered above will be stable

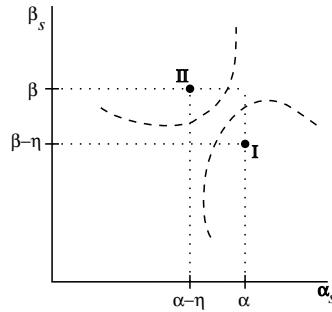


Fig. 1. Schematic representation in the parameter space (α_s, β_s) of the regions where synchronization with lag-time Δ_I and Δ_{II} occur.

on two different ranges of the coupling constant η . If the master map is chaotic, we expect that for sufficiently small and large η full synchronization is unstable and stable in both cases, respectively, while for intermediate values only one of the cases admits full synchronization.

We have seen above that full synchronization is possible at two points in the (α_s, β_s) parameter space, with different lag-times in each case. To encounter such synchronized states, the slave-map parameters must be exactly tuned on one of those synchronization points. Their location is schematically shown in Fig. 1. Though when the slave system is slightly detuned with respect to the synchronization points full synchronization will not occur, it is expected that the slave-map orbit follows approximately the master-map orbit with the same lag-time, Δ_I or Δ_{II} . To quantitatively characterize the degree of synchronization between the two orbits and the respective lag-time, we may use the so-called similarity function S_Δ , defined as

$$S_\Delta^2 = \frac{\langle [x_{n+\Delta} - y_n]^2 \rangle}{[\langle x_n^2 \rangle \langle y_n^2 \rangle]^{1/2}}, \tag{13}$$

where the brackets $\langle \cdot \rangle$ stand for time averages over asymptotically large times. If x_n and y_n are independent time series with similar mean value and dispersion we have $S_\Delta \approx \sqrt{2} \approx 1.4$. If, on the other hand, there is full synchronization with lag-time Δ , $S_\Delta = 0$. The similarity function S_Δ can be determined, at each point (α_s, β_s) in parameter space and for each lag-time Δ . At $(\alpha, \beta - \eta)$, we should have $S_{\Delta_I} = 0$, while at $(\alpha - \eta, \beta)$ we should have $S_{\Delta_{II}} = 0$. It is expected, moreover, that in a region around each synchronization point the similarity function attains a minimum, as a function of the lag-time, for $\Delta = \Delta_I$ and $\Delta = \Delta_{II}$, respectively. These regions are qualitatively illustrated in Fig. 1. In the remaining of the parameter space, as far as the slave-map orbits do not diverge, the similarity function can attain a minimum for any other value of Δ —without reaching, however, $S_\Delta = 0$. Note that the boundaries of such regions will in general depend on the coupling constant η . In the following sections, we study these aspects of synchronization in Eqs. (5) and (6) for logistic and Hénon delay maps in their chaotic regime.

3. Synchronization of delayed logistic and Hénon maps

3.1. Logistic maps

As a first illustration of the synchronization properties of Eqs. (5) and (6) in cases I and II, we consider the choice $f(x) = x(1 - x)$ and $g(x) = 0$. The master system becomes a delayed logistic map

$$x_{n+1} = \alpha x_n(1 - x_n) + \beta x_{n-n_1}(1 - x_{n-n_1}), \quad (14)$$

whose orbits are bounded to the interval $(0, 1)$ for $0 < \alpha, \beta$ and $\alpha + \beta \leq 4$. In different regions of the parameter space (α, β) and depending on the delay n_1 , this system displays periodic, quasiperiodic and chaotic evolution. The corresponding slave map is given by

$$y_{n+1} = \alpha_s y_n(1 - y_n) + \beta_s y_{n-n_1}(1 - y_{n-n_1}) + \eta x_{n-n_2}(1 - x_{n-n_2}). \quad (15)$$

Its orbits are nondivergent for $0 < \alpha_s, \beta_s, \eta$ and $\alpha_s + \beta_s + \eta < 4$.

Fig. 2 displays the synchronization regions in the parameter space (α_s, β_s) and how they vary as the coupling coefficient η increases. The master map parameters are $\alpha=1.8$, $\beta=2.1$ and the delay times are $n_1=2$, $n_2=3$. For each pair (α_s, β_s) we have determined S_A as a function of the lag-time A , and detected the value of A for which the similarity function attains its minimum $\min(S_A)$. The left column of Fig. 2 displays this minimum for three values of η . Light tones represent low values of $\min(S_A)$, i.e., high master–slave correlation, while darker tones correspond to poor correlation [$\min(S_A) \sim 1$]. In the black upper-right region the slave-map orbits diverge.

The right column of Fig. 2 displays the lag-time A at which the similarity function attains its minimum. The region where S_A is minimal with lag-time $A_I = n_2 - n_1 = 1$ is represented by the darker gray tone, while the region with lag-time $A_{II} = n_2 = 3$ is represented by the lighter gray tone. White represents the parameter region where the minimum value of the similarity function occurs for a lag-time which is different from A_I or A_{II} . Black represents the parameter region where the trajectory of the slave map diverges.

For low coupling intensity, $\eta = 0.2$, both synchronization regimes are unstable (Figs. 2(a) and (b)). The synchronization regions are not well defined and have fuzzy boundaries. While the minimum of the similarity function at point I occurs at the expected lag-time A_I , the minimum of the similarity function at point II occurs at a different lag-time. Notice, in fact, that in Fig. 2(b) point II is in the white region that represents a lag-time different from A_I or A_{II} . The region corresponding to each regime is disconnected and quite complex in shape, with parts in distant zones of the parameter space. Note, for instance, the light-gray zones near $\beta_s = 0$ where master–slave correlation is however rather poor.

As the coupling intensity grows, zones I and II become more uniform and increase in total extension. For $\eta = 0.8$, only regime I is stable (Figs. 2(c) and (d)). In this case, $\min(S_A)$ at points I and II is equal to 0 and 0.2, respectively. For large enough η ,

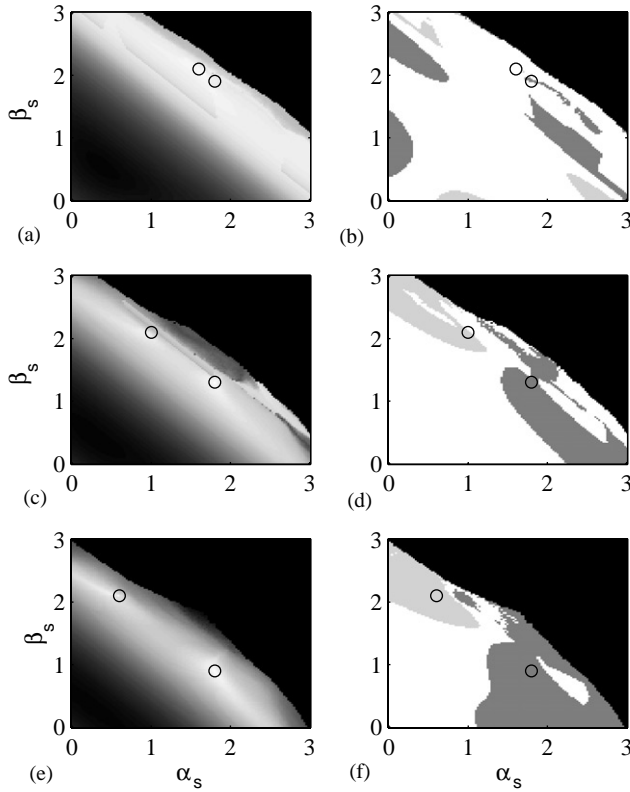


Fig. 2. Synchronization regions in the (α_s, β_s) parameter space in the case of the logistic map, for increasing coupling: ((a), (b)) $\eta = 0.2$; ((c), (d)) $\eta = 0.8$; ((e), (f)) $\eta = 1.2$. The master map parameters are $\alpha = 1.8$, $\beta = 2.1$, and the delay times are $n_1 = 2$ and $n_2 = 3$. The left column displays the minimum of the similarity function. Light tones represent low values of $\min(S_A)$ (good master–slave correlation) and vice versa. Black represents the region where the slave-map trajectories diverge. The right column displays the lag-time where the minimum value of S_A occurs. In the light-gray region, the lag-time is $\Delta_{II} = n_2 = 3$, while in the dark-gray region it is $\Delta_I = n_2 - n_1 = 1$. In the white region, the lag-time is different from Δ_I or Δ_{II} . The small circles stand at the synchronization points I and II, $(\alpha_s = \alpha, \beta_s = \beta - \eta)$ and $(\alpha_s = \alpha - \eta, \beta_s = \beta)$, respectively.

both regimes are stable (Figs. 2(e) and (f); $\eta = 1.2$) and, as expected, $\min(S_A)$ equals zero at points I and II.

Fig. 3 illustrates the master–slave correlation at different points of parameter space for $\eta = 1.0$ (all other parameters are as in Fig. 2). In this case, type I synchronization is stable (Fig. 3(a)) but type II is not (Fig. 3(b)), and it is worth mentioning that the minimum value of the similarity function, $S_A = 0.057$, does not occur at point II ($\alpha_s = 0.8, \beta_s = 2.1$) but at a point close to it ($\alpha_s = 0.75, \beta_s = 2.1$). Fig. 3(c) displays the correlation plot at a point where the lag-time at which S_A attains its minimum is $\Delta = -15$.

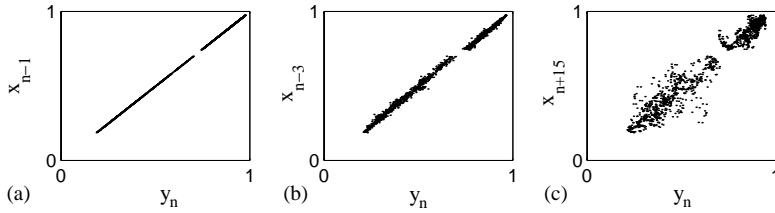


Fig. 3. Correlation plots for $\eta = 1.0$, $n_1 = 2$, $n_2 = 3$ and (a) $\alpha_s = 1.8$, $\beta_s = 1.1$, $\min(S_A) = 0$; (b) $\alpha_s = 0.75$, $\beta_s = 2.1$, $\min(S_A) = 0.057$; (c) $\alpha_s = 1.25$, $\beta_s = 1.525$, $\min(S_A) = 0.25$. The master-map parameters are as in Fig. 2.

3.2. Hénon maps

As a second example, we study now a master–slave configuration where each element is a two-dimensional delay map, namely, a Hénon-like map. The evolution of the master coordinates $\mathbf{x}_n = (u_n, v_n)$ is given by the functions $\mathbf{f}(\mathbf{x}) = (-u^2, 0)$ and $\mathbf{g}(\mathbf{x}) = (1 + v, bu)$, so that the master system is

$$\begin{aligned} u_{n+1} &= 1 - \alpha u_n^2 - \beta u_{n-n_1}^2 + v_n, \\ v_{n+1} &= b u_n, \end{aligned} \tag{16}$$

cf. Eq. (5). In the following, we choose $b = 0.3$. The slave system, with coordinates $\mathbf{y}_n = (w_n, z_n)$, is governed by the equations

$$\begin{aligned} w_{n+1} &= 1 - \alpha_s w_n^2 - \beta_s w_{n-n_1}^2 + z_n - \eta u_{n-n_2}^2, \\ z_{n+1} &= b w_n, \end{aligned} \tag{17}$$

so that coupling acts on the first coordinate only. The synchronization manifold is given by

$$\begin{aligned} w_n &= u_{n+n_3-n_2}, \\ z_n &= v_{n+n_3-n_2}, \end{aligned} \tag{18}$$

where, as before, $n_3 = n_1$ in case I and $n_3 = 0$ in case II.

Next, we study in which regions of parameters the different synchronization regimes occur. We take parameters for the master map α, β, n_1 such that its dynamics is chaotic.

Fig. 4 displays the minimum of the similarity function and the lag-time for which the minimum occurs, in the parameter space (α_s, β_s) . The results are similar to those found with the logistic map. For weak coupling the synchronization regions are not well defined, but as the coupling increases their size grows and the boundary between them becomes well defined. For large η both synchronization regimes are stable. Thus, it can be thought that a small variation of the slave-map parameters α_s or β_s near the boundary region might induce a transition from synchronization with lag-time Δ_I to synchronization with lag-time Δ_{II} or vice versa. However, near the boundary region we find $\min(S_A) \approx 0.5$, which indicates bad synchronization. Therefore, while the lag-time

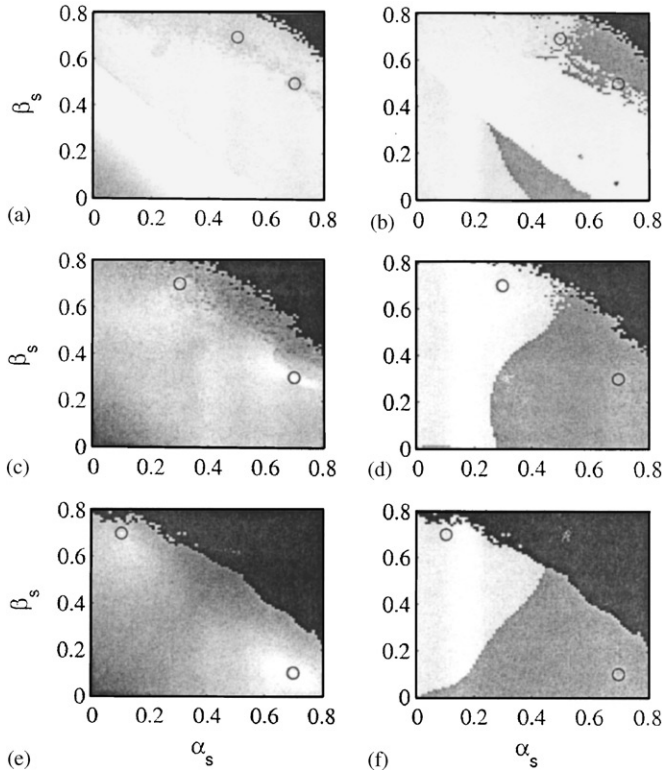


Fig. 4. Synchronization regions for delayed Hénon maps. The parameters of the master map are $\alpha = 0.7$, $\beta = 0.7$, and delay times are $n_1 = 6$ and $n_2 = 3$. The left column displays the minimum of the similarity function and the right column displays the lag-time where $\min(S_A)$ occurs. In the light-gray region, the lag-time is $\Delta_{II} = n_2 = 3$, while in the dark-gray region it is $\Delta_I = n_2 - n_1 = -3$. In the white region of (b) the lag-time is different from Δ_I or Δ_{II} . The small circles indicate the points $(\alpha_s = \alpha - \eta, \beta_s = \beta)$, and $(\alpha_s = \alpha, \beta_s = \beta - \eta)$. ((a), (b)) $\eta = 0.2$; ((c), (d)) $\eta = 0.4$; ((e), (f)) $\eta = 0.6$.

at which the minimum value of S_A occurs changes abruptly (from Δ_I to Δ_{II}), there is no sharp transition between one regime of synchronization to the other. If the slave-map parameters are gradually modified from points I to II, synchronization with lag-time Δ_I is gradually lost, and as we enter region II, synchronization with lag-time Δ_{II} is gradually established.

4. Conclusion

We have studied two regimes of synchronization of delayed nonidentical maps. We have shown analytically that, by suitably tuning the slave-map parameters, two distinct synchronization regimes can occur. In one regime, the lag-time between the slave and the master maps is given by the delay of the coupling, n_2 , while in the other regime

is given by the difference between the delays, $n_1 - n_2$. We have also shown that these two regimes are actually two particular cases of synchronization with a slave map that is identical to the master map but that has two delayed feedback terms.

The two synchronization regimes have been exemplified by considering delayed logistic and Hénon maps. In both cases, the synchronization regimes are simultaneously stable only for large values of the coupling η , and therefore, they occur at parameters of the slave map, (α_s, β_s) , which are far away from each other. In other words, our results show that in the case of delayed logistic and Hénon maps, a small variation of a parameter of the slave map cannot induce a transition from regime I to regime II or vice versa, since they occur in distant regions of the parameter space. On the contrary, in the case of semiconductor lasers with optical feedback, it has been shown numerically [19,21] that close to the lasing threshold, by carefully tuning a parameter of the slave laser one can induce a transition from one regime of synchronization to the other. It will be interesting to study a delayed map that shows this type of transition, and allows an analytical investigation of the phenomenon.

Acknowledgements

This work was supported by Proyecto de Desarrollo de Ciencias Básicas (PEDECIBA) and by Comisión Sectorial de Investigación Científica (CSIC), Uruguay.

References

- [1] N. MacDonald, *Biological Delay Systems: Linear Stability Theory*, Cambridge University Press, Cambridge, 1989.
- [2] J. Foss, A. Longtin, B. Mensour, J. Milton, *Phys. Rev. Lett.* 76 (1996) 708.
- [3] B. Mensour, A. Longtin, *Phys. Rev. E* 58 (1998) 410.
- [4] K. Ikeda, K. Matsumoto, *Physica D* 29 (1987) 223.
- [5] J.-P. Goedgebuer, L. Larger, H. Porte, *Phys. Rev. Lett.* 80 (1998) 2249.
- [6] V.S. Udaltsov, J.-P. Goedgebuer, L. Larger, W.T. Rhodes, *Phys. Rev. Lett.* 86 (2001) 1892.
- [7] H.U. Voss, *Phys. Rev. E* 61 (2000) 5115.
- [8] V. Ahlers, et al., *Phys. Rev. E* 58 (1998) 7208.
- [9] C. Masoller, *Phys. Rev. Lett.* 86 (2001) 2782.
- [10] S. Sivaprakasam, et al., *Phys. Rev. Lett.* 87 (2001) 154 101.
- [11] Y. Liu Y, et al., *Appl. Phys. Lett.* 80 (2002) 4306.
- [12] A. Murakami, J. Ohtsubo, *Phys. Rev. A* 65 (2002) 033 826.
- [13] F. Rogister, et al., *Opt. Commun.* 207 (2002) 295.
- [14] R. Vicente, T. Perez, C.R. Mirasso, *IEEE J. Quantum Electron.* 38 (2002) 1197.
- [15] H.U. Voss, *Phys. Rev. Lett.* 87 (2001) 014 102.
- [16] C. Masoller, D.H. Zanette, *Physica A* 300 (2001) 359.
- [17] A. Locquet, F. Rogister, M. Sciamanna, P. Mégret, M. Blondel, *Phys. Rev. E* 64 (2001) 045203(R).
- [18] A. Locquet, C. Masoller, P. Mégret, M. Blondel, *Opt. Lett.* 27 (2002) 31.
- [19] I.V. Koryukin, P. Mandel, *Phys. Rev. E* 65 (2002) 026 201.
- [20] E.M. Shahverdiev, S. Sivaprakasam, K.A. Shore, *Phys. Lett. A* 292 (2002) 320.
- [21] A. Locquet, C. Masoller, C.R. Mirasso, *Phys. Rev. E* 65 (2002) 056 205.
- [22] S. Sivaprakasam, et al., *Opt. Lett.* 27 (2002) 1250.
- [23] S. Sivaprakasam, et al., *IEEE J. Quantum Electron.* 38 (2002) 1155.